

EXPERIMENTAL AND NUMERICAL INVESTIGATIONS ON POLYCARBONATE SAMPLES AND ROTORCRAFT WINDSHIELD FOR BIRD MODEL IMPACTS

Janusz ĆWIKLAK¹, Paweł GOLDA², Artur GOŚ³, Ewelina KOBIALKA⁴, Kamil KRASUSKI⁵

^{1, 3, 4, 5} Institute of Navigation, Polish Air Force University, Dęblin, Poland

² Faculty of Aviation, Polish Air Force University, Dęblin, Poland

Abstract:

One of the factors that significantly affect flight safety is bird strikes. Various aircraft parts are vulnerable to damage. For helicopters, the windshield, the front part of the fuselage, and the rotor blades are particularly sensitive to bird collisions. Experimental studies and numerical modelling of bird model impacts on polycarbonate samples and a helicopter windshield are presented in the paper. For the tests, a gelatine projectile was used as a bird substitute. In numerical studies, it was represented by a cylindrical shape with hemispherical ends. In the first stage of the experimental tests samples made of polycarbonate material were used as a target. These studies focused on determining the sample deflections and velocity at which the bird model would penetrate the target. The experimental investigations were conducted with a special set-up of a gas gun equipped with high-speed cameras, tensiometers, accelerometers, and force sensors. The simulations were conducted using LS-DYNA software by applying the SPH method to the bird model. The test stand models were developed in a CAD environment and then imported into LS-PrePost software, where they were discretized to use in numerical analyses. Results of the studies, such as impact force, acceleration, and windshield deflection were compared. Besides, the high-speed cameras allowed visualization of the impact process. It turned out that both a polycarbonate plate and a helicopter windshield were punctured at the speed of 50 m/s. It can be noted that the curves of the impact force and the deflection of samples obtained as a result of numerical analysis correlated well with the empirical ones. The correlation validated the modelling parameters and confirmed that numerical simulations could be trusted as an effective and reliable method for analyzing materials' behavior under impact loading.

Keywords: bird strikes, bird models, experimental tests, numerical simulations, helicopter windshield

To cite this article:

Ćwiklak, J., Golda, P., Goś, A., Kobialka, E., Krasuski, K., (2024). *Experimental and numerical investigations on polycarbonate samples and rotorcraft windshield for bird model impacts*. Archives of Transport, 70(2), 79-96. <https://doi.org/10.61089/aot2024.eea5zs04>



Contact:

1) j.ewiklak@law.mil.pl, [https://orcid.org/0000-0001-5538-0440] - corresponding author, 2) p.golda@law.mil.pl, [https://orcid.org/0000-0003-4066-7814], 3) a.gos@law.mil.pl, [https://orcid.org/0000-0002-4268-8830], 4) e.kobialka@law.mil.pl, [https://orcid.org/0000-0001-5177-8144], 5) k.krasuski@law.mil.pl, [https://orcid.org/0000-0001-9821-4450]

1. Introduction

Aviation safety depends on many factors. One of them is bird strikes, which negatively impact on flight safety (Dhillon, 2011; McIntyre, 2017; Metz, 2021). Various parts of an aircraft are subjected to damage (Dolbeer et al., 2021). It goes without saying that damage to an engine, as well as windshield penetration, is extremely dangerous. The consequence of a bird being sucked into an engine can be the engine shutting down, whereas the penetration of the canopy can cause serious injury to the pilot, making them unable to continue piloting the aircraft (El-Sayed, 2019). In order to comply with certification requirements regarding the resistance of various parts of an aircraft to bird impacts, compulsory experimental tests must be conducted (Heimbs, 2011; Guida, et al., 2013).

The legal regulations concerning the strength requirements for the aircraft and rotorcraft windshield include the specification CS-25 and CS-29. According to these specifications, the windshield in the category of a heavy aircraft and rotorcraft should withstand a bird strike whose mass equals 1 kg at a speed of 180 km/h, and an altitude of 2438 m. (EASA, CS-25, CS-29, 2011). However, there are no requirements regarding the categories of small aircraft (CS-23) and rotorcraft (CS-27). As the statistics show, there were many accidents concerning this category where the windshield was damaged due to a bird strike (Dennis and Lyle, 2009; El-Sayed, 2019). It can be assumed that one of reasons of that was the lack of certifying requirements. The Figure 1 depicts an example of the windshield damages of diamond DA42 plane as a result of bird strike. The accident occurred during the approach to landing at the Dęblin airport on September 25, 2020. The strike speed was approximately 80 kt (41 m/s). A pigeon was the impactor. Therefore, the main aim of the paper is the comparison of the experimental and numerical results which is needed for further numerical analysis in order to develop the more resist on bird strikes innovative windshield models intended for aircraft of the category "small".

It is important to underline, that experimental tests conducted on the subject often constitute a manufacturer's trade secret, thus the number of available papers regarding experimental tests of bird strikes is very limited. Moreover, experimental tests are very expensive and time consuming. Therefore, the ma-

jority of researchers conducting numerical simulations of bird strikes exploit the data of published studies, especially Wilbeck's and Barber's, which were carried out in the 1970s. Furthermore, the conducted tests are unique from the Polish perspective and can popularize the problematic in the national research centers.

Taking into account the above mentioned circumstances, the experimental tests conducted by authors are valuable and may serve as a reference for other researches. We believe, that results of the studies presented in the manuscript will constitute new research and will be of interest to researchers.



Fig. 1. Damaged windshield of DA-42 after bird strike (courtesy of Marta Kuzyka)

Therefore, it seems justified to conduct the tests and numerical simulations of bird strike in order to seek

new solutions regarding windshield construction. Within the conducted analyses the impact loaded object was the SW-4 helicopter windshield and samples made of polycarbonate panels. The experimental tests were carried out using a special gas cannon. The test stand was equipped with cameras, strain gauges, force sensors and accelerometers (Ćwiklak et al., 2022). LS_DYNA software package was applied for conducting numerical analysis (LSTC, LS-DYNA, 2007). The Introduction part describes the purpose of the article, the justification for the scientific research carried out, as well as its contribution to the development of air transport safety. The second part of the article describes the experimental and numerical methods that were used during the research. The next part contains research results in the form of graphs and drawings from experimental and numerical tests. The last part of this paper presents a summary, conclusions and plans for future research on bird strikes.

2. Literature review

Two general categories can be distinguished among experimental tests. The first group involves validation of bird models through impacting them into a rigid plate (Barber, 1978; Allaey, et al., 2017), whereas the second group involves impacting the substitute bird into various parts of an aircraft in order to comply with EASA or FAA safety requirements and to find new materials resistant to bird strikes. (Wilbeck, 1977; Liu, et al., 2014; Hedayati and Sadighi, 2015).

Researchers have conducted a number of experimental and numerical studies to analyze the impact resistance of a variety of aircraft parts, including windshields, flaps, and fan blades. (Yang et al., 2003; Wang and Yue, 2010; Ivančević and Smojver, 2011; Dar et al., 2013; Hedayati, et al., 2014; Jin, 2014; Liu, et al., 2014; Plassarda, et al., 2015; Vijayakumar, et al., 2015; Delsart, et al., 2017; Husainie, 2017; Orlando, et al., 2018; Zhou et al., 2019; Zhou et al., 2020; Arachchige, et al., 2020; Di Caprio, et al., 2020; Pernas-Sánchez, et al., 2020; Wu, et al., 2021). Despite this, no information regarding the set-up used in the published studies is available. An example of a comparison between the experimental and numerical investigations regarding windshields (a polycarbonate plate of 8 mm in thickness) has been presented in studies (Plassarda et al., 2015). A dead chicken was used as an bird

model impacting with a windshield. The impact velocity was 128 m/s. The values of the contact force and the deflection were recorded and compared to numerical analyses. A deep deflection of the polycarbonate plate and an its elastic behavior were observed. It could be stated that the polycarbonate plate is a flexible material (Plassarda et al., 2015; Ćwiklak, 2020).

3. Methods

The figure 2 shows a step by step a research methodology of conducting of the experiment and numerical analyses.

The first step was preparing the different samples (different thickness, single-layer, multi-layers) and projectiles. Next, the testing sample was mounted on the frame of the stand. Parameters of the test, such as a velocity and mass of the projectile were set. Each shot was conducted after placing the gelatine projectile in the barrel. After the shot recorded parameters were analysed. Numerical bird models and polycarbonate samples were elaborated in Solid works and LS-PrePost software. In the next step was performing numerical computing by Ls-Dyna solver. After that, the results obtained from the test were compared with numerical ones. In a case, in that the values of analysed parameters were comparable, the results were recorded and sending to further analyses. Otherwise, numerical models were improved and the process of analysis were repeated.

3.1. Experimental method

The experimental tests of bird impact with polycarbonate plates and helicopter windshield were carried out at the Institute of Aviation in Warsaw. The dedicated test stand consisted of the following elements:

- air pressure gun;
- multi-channel recorder (LMS SCADAS Mobile SCR09);
- force sensors (M204C PCB) - 4 pcs;
- strain gauges;
- acceleration gauge;
- portable computer equipped with LMS Test.XPress software – measurement control, data recording and archiving;
- a desktop computer to control a gas gun equipped with Gun Control software;
- high speed camera (Phantom VEO 412L + TAMRON 28-75 mm);

- left high speed camera (Phantom V1612 + NIKON 70-300 mm);
- right high speed camera (Phantom V1612 + NIKON 105 mm);
- computer with PCC 3.1 camera software.

The scope of the measurements included:

- measurement of projectile speed;
- measurement of impact force with four sensors;
- measurement of strains;
- displacement of samples;
- accelerations.

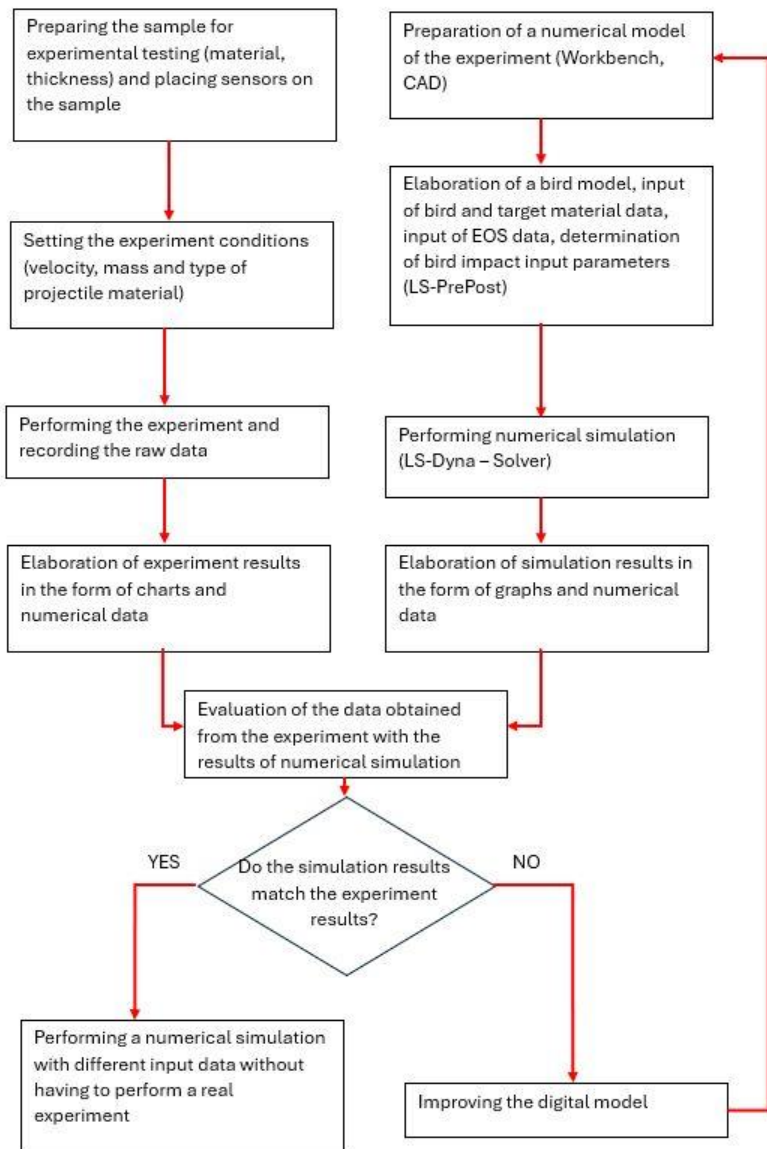


Fig. 2. Research methodology flowchart

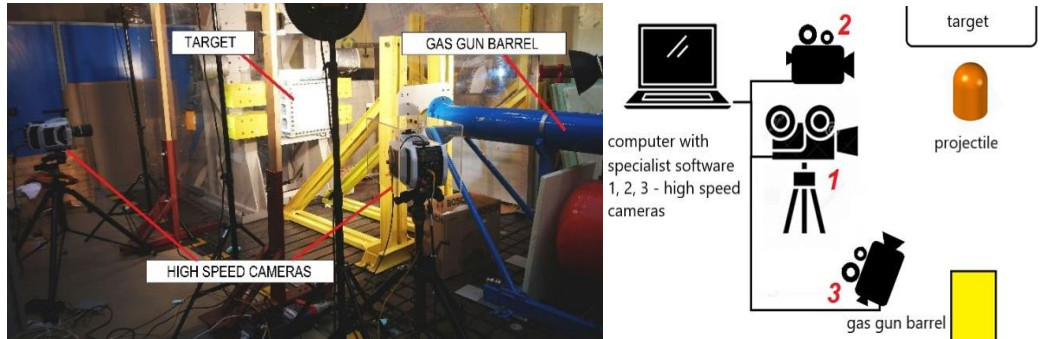


Fig. 3. Experimental setup elements

An illustration of the experimental setup elements that were used during polycarbonate samples tests is shown in Figure 3. For the purpose of determining the projectile velocity, camera number one was used. The target displacement was recorded by camera number 2. The impact process was observed using camera number 3.

The rear montage plate is made of a 0.01 m thick square rigid plate (0.5×0.5m) mounted with four bolts supported by 4 load sensors (Figure 4a). Four distance elements are fixed to the rear montage plate. Material samples for testing are fixed to distance elements with 40 screws (10 for each side of the sample). Figure 4b presents the tested polycarbonate plate mounted on the frame of the test stand. The force sensors and strain gauges were connected to the data recorder. To initiate a shot from the DPZ-

250 gas gun, the technician used a trigger connected to cameras and data recorders. Additionally, the trigger ensured time synchronization across all devices. As shown in Figure 4c, four markers were used to record the sample deflection.

3.2. Numerical methods

In order to conduct a numerical analysis of a bird impact into a rigid and deformable target, the LS-DYNA software package was used (LSTC, LS-DYNA, 2007). This is a computational code designed to analyze fast-changing phenomena by means of the finite-element method. A quick explicit formulation has been chosen for the research. Additionally, in order to elaborate bird and target models LSPre-Post software was exploited.

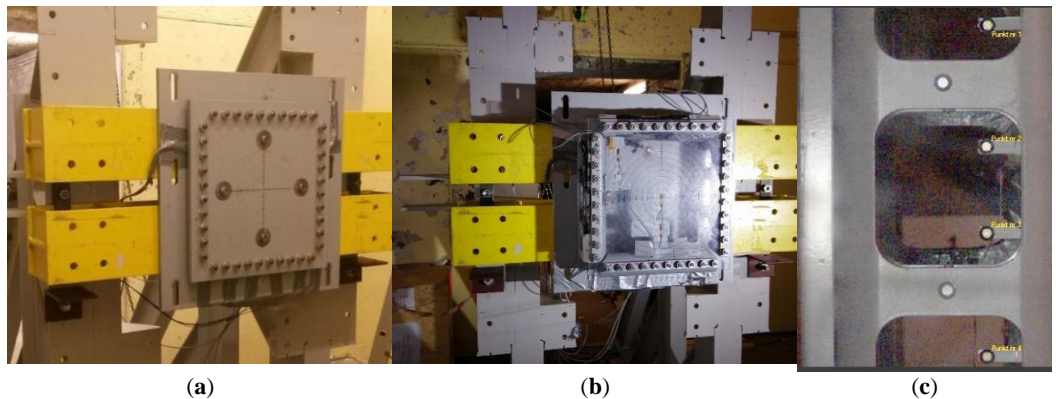


Fig. 4. Parts of experimental setup: (a) load sensors; (b) polycarbonate plate; (c) four markers used for recording of the sample deflection

Within this article a bird, 1.0 kg in mass and in a cylindrical shape with hemispherical ends ($D = 0.094$ m; $L = 2D = 0.188$ m) was modelled with the SPH method (Figure 5) (McCarthy et al., 2010; Lyu et al., 2022; Roper-Giralda et al., 2021; Lacombe, 2004; Kalam et al., 2017; Zhang et al., 2018; Zhu et al., 2021). The dimensions of the bird models have been determined on the basis of the adopted bird mass and material density (Hedayati and Ziaei-Rad, 2012). The bird model consists of 35.820 elements with distance between SPH elements of 3 mm (pitch value 3 mm) (Guida et al., 2011; Soni et al., 2013; Fragrasa et al., 2019). This model was chosen for the simulation presented in this paper since it reflected the behavior of a gelatin projectile more accurately during experimental tests than others (Ćwiklak et al., 2022).

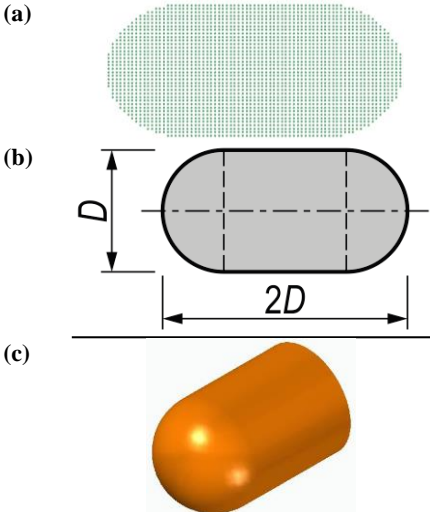


Fig. 5. Shape and dimensions of SPH bird model and the gelatin projectile

As a material for the bird model, a plastic-elastic hydrodynamic material was taken from the LS-DYNA material base. Under impact at speeds less than 100 m/s, this material better represents bird behavior than the null material. Thus, for numerical analyses of bird strikes, applying the right EOS during model design is essential. In the research, Grüneisen's EOS has been applied (Chuan, 2006; Heimbs, 2011). The form of the equation of state are given below.

$$p = \rho_0 C^2 \mu \left\{ \frac{[1 + (1 - \frac{\gamma_0}{2})\mu - \frac{a}{2}\mu^2]}{[1 - (S_1 - 1)\mu - S_2 \frac{\mu^2}{\mu + 1} - S_3 \frac{\mu^3}{(\mu + 1)^2}]^2} \right\} + (\gamma_0 + a\mu)E, \quad (1)$$

where: E is the internal energy per initial volume, C is the intercept of the $u_s - u_p$ curve, S_1 , S_2 and S_3 are the coefficients of the slope of the $u_s - u_p$ curve, γ_0 is the Grüneisen gamma, a is the first order volume correction to γ_0 . Constants C , S_1 , S_2 , S_3 , γ_0 and a are user defined input parameters. The compression is defined in terms of the relative volume V , as:

$$\mu = \frac{1}{V} - 1 \quad (2)$$

For expanded materials as the pressure is defined by:

$$p = \rho_0 C^2 \mu + (\gamma_0 + a\mu)E \quad (3)$$

In order to digitally model the samples and the windshield a material model from the LS Dyna software database was used. The material model used is: elastic plastic with kinematic hardening. In the implementation of this material model of polycarbonate samples and the windshield, the deviatoric stresses are updated elastically:

$$\sigma_{ij}^* = \sigma_{ij}^n + C_{ijkl} + \Delta \varepsilon_{kl} \quad (4)$$

where:

σ_{ij}^* - is the trial stress tensor,

σ_{ij}^n - is the stress tensor from the previous time step,

C_{ijkl} - is the elastic tangent modulus matrix,

$\Delta \varepsilon_{kl}$ - is the incremental strain tensor.

If the yield function is satisfied, nothing else is done. If, however, the yield function is violated, an increment in plastic strain is computed, the stresses are scaled back to the yield surface, and the yield surface center is updated (Livermore Software Technology Corporation, 2007)

Table 1 presents material and EOS parameters adopted in the bird model. A preliminary test was carried out with a plexiglass plate with dimensions of $0.5 \times 0.5 \times 0.01$ m (flexible target) in order to check the behavior of both the gelatin bird model and the deformation of the flexible plate. Material data for the targets mentioned are listed in Table 2.

Table 1. Material and EOS data used in bird models (Ćwiklak, 2020)

Material parameters of bird model				
Density	Cut-off pressure	Shear modulus	Yield stress	Failure strain
[kg/m ³]	[Pa]	[Pa]	[Pa]	[-]
950	-10 ⁶	3.500x10 ⁹	10 ⁶	0
Grüneisen's EOS parameters				
Bulk speed of sound	Linear coefficient	Quadratic coefficient	Cubic coefficient	Grüneisen's gamma
[m/s]	[-]	[-]	[-]	[-]
1.438	1.92	0	0	0.1

Table 2. Material data used in targets

Data of polycarbonate plate and the windshield material (0.5×0.5×0.004 m)						
Density	Young's modulus	Poisson's ratio	Yield stress	Failure strain	Tangent modulus	Hardening parameter
[kg/m ³]	[Pa]	[-]	[Pa]	[-]	[Pa]	[-]
1.190	3200·10 ⁶	0.35	6000·10 ⁷	0.025	-	0.5

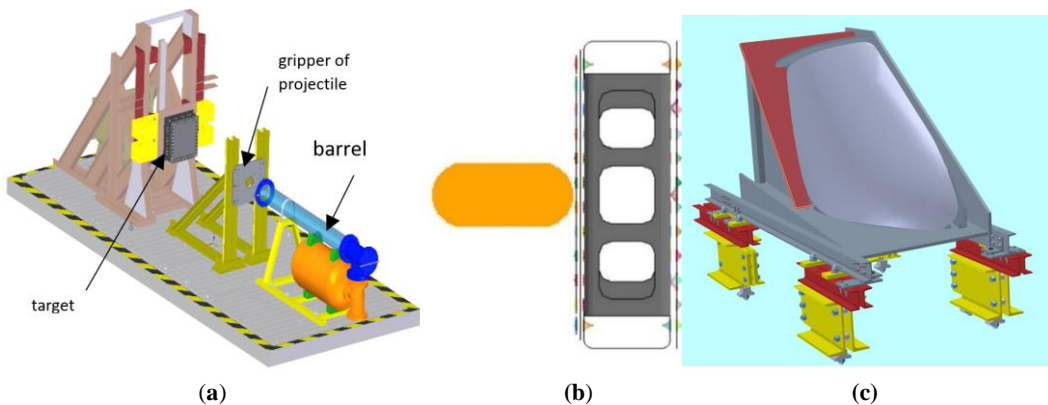


Fig. 6. FE model of the stand test (a); the position of the bird model in the initial moment of analysis (b); numerical model of the stand to fix the windshield (c)

Model of the test stand presented in Figure 6 was developed in CAD environment and then imported into LS-PrePost software, where it was discretized for numerical analysis. Similar to the stand, four bolts, supported by 4 load sensors, connect the target with other elements of the stand. The bolts were grouped in the single point constraints (SPC) set and all the translational degrees of freedom in x, y, z directions were constrained. In this case an SPC boundary condition card was chosen. This setup provided the same boundary conditions for the experimental tests and numerical simulations. Furthermore, it allowed the researchers to measure

the SPC force, as in the experimental tests. The contact automatic nodes to surface was adapted. The function of the master segment was taken by the target, whereas the slave segment was a bird model. The contact automatic single surface was used as the contact between the target and others parts of the stand.

In the comparisons a steel, rigid plate was used as the target. The tests were conducted at speed of 116 m/s (Ćwiklak et al., 2022. One of the parameters recorded during the experimental tests was the impact force (Figure 7). The impact force diagram obtained in the experiment was compared with the

force obtained from the simulation. When analyzing the course of the curves, it can be concluded that their shapes are comparable and their maximum values correlate well with each other. It means that SPH bird model reflects the behavior of the gelatin model accurately and can be exploited for numerical analyses regarding the bird impact with polycarbonate samples or the helicopter windshield.

During the experimental tests, two shots involved a gelatine projectile hitting a plexiglass plate, which was a flexible target. The main aim was to assess both the behavior of the gelatin bird model and the flexible target during the impact process (Figure 8). It was a preliminary investigation before further experimental and numerical studies regarding aircraft windshields.

Table 3. Initial simulation parameters

Initial simulation parameters	Description
Element type of bird models	SPH elements
Element type of the rigid plate (target)	Belytschko-Tsay shell elements
Contact type	Automatic nodes to surface Automatic single surface
Hourglass control	Flanagan-Belytschko viscous form (IHQ=2) Coefficient (QM=0.4)
Bulk viscosity control	Quadratic viscosity coefficient (Q1=2.0) Linear viscosity coefficient (Q2=0.25)
Time step	6×10^{-6} s
Initial velocity	50-80 m/s
The analysis time	5-15 s

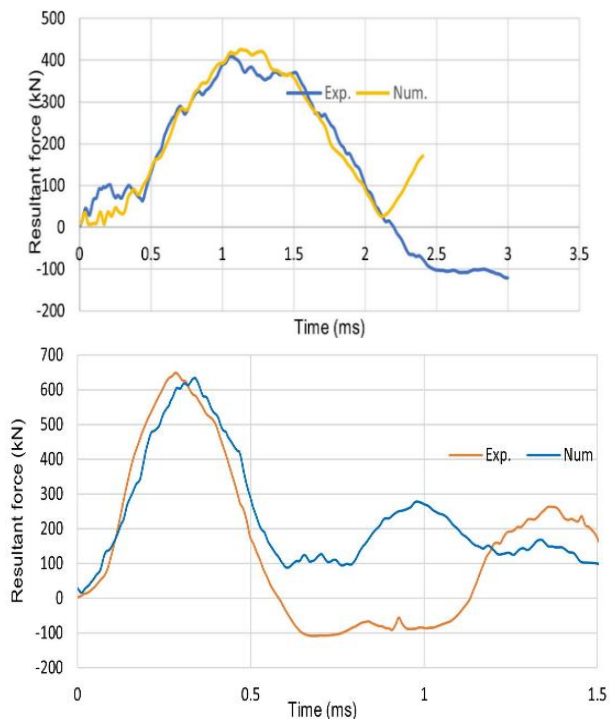


Fig. 7. Comparison of the resultant forces obtained from experimental and numerical analyses

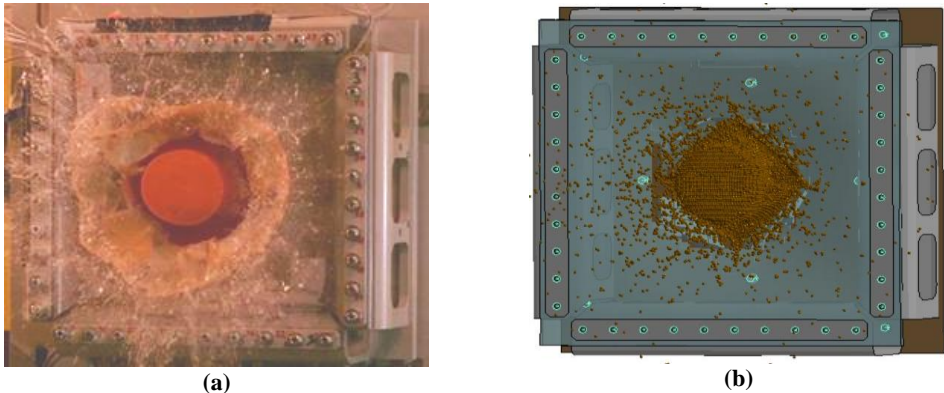


Fig. 8. Comparison of the projectile and the plexiglass plate deformations for experimental (a) and numerical (b) studies

In regards to the behavior of the plexiglass plate, numerical simulations show that the plexiglass plate is more elastic in comparison to experiment, which shows that it is more brittle (Zochowski et al., 2022).

4. Results and discussion

In this section, the results of both experimental tests and numerical analyses are presented. The experimental tests concerned the impact of the gelatin projectile on the polycarbonate panels 4 mm thick at a speed of about 50 m/s. The shot into the helicopter windshield was the next stage of the tests.

Figure 9 shows the impact of the gelatine projectile on the polycarbonate sample. Characteristic moments have been chosen to illustrate the deformation process between the impactor and the target. After about 3 ms, the impactor punctured the sample. To confirm the moment of plate breaking, the resultant forces obtained from experimental and numerical studies were compared. Figure 10 shows plots of forces. According to the curves, the maximum values of the forces are approximately 45 kN and the courses of the curves are similar. Figure 11 shows the comparison of the polycarbonate plate deflection from the experiment and the simulations. The displacement was recorded at four different points used for tests and simulations.

Analyzing the displacement values of the polycarbonate samples it can be seen that those values are similar for the test and the simulation. The deflection values equal about 50 mm at a time 3 ms after impact. As mentioned above, at this time the sample was punctured (Figure 9c). The analyzed points were located in the center of the samples. The next

point was 100 mm above the center of each sample. As a result, the deflections were smaller and equal to 28 mm and 30 mm, respectively. It is pertinent to underline that the sample displacement was recorded at 4 points with markers (Fig 4c). After the shot, due to the sample damage, two markers were damaged too, so the displacement could not be recorded.

In Figure 12, an interesting comparison is shown between accelerations observed in tests and simulations. For the test and the simulation, the maximum values of acceleration at a time of about 0.25-0.3 ms after impact are almost the same (40000 m/s²). However, curves have different courses. In the experimental test acceleration rapidly decreases to zero, while in the simulation it comes down and oscillates around 10000 m/s². It could be caused by the lower sensitivity of the acceleration sensor. The next difference is the rapid rise at the moment of rupture of the sample. In the test, the acceleration equals 80000 m/s², while in the simulation it is about 55000 m/s².

Next, experimental tests were conducted regarding the impact of gelatin projectiles on helicopter windshield. To conduct the mentioned tests, a dedicated stand was constructed. A frame for fixing the windshield was made from plywood and mounted on the main part of the stand. To record the resultant forces, four load sensors were attached to this device.

In order to record the displacement of the windshield in chosen points 10 markers were fixed (Fig. 13a). Figure 13 b presents the windshield on test stand with mounted markers, and tensiometers.

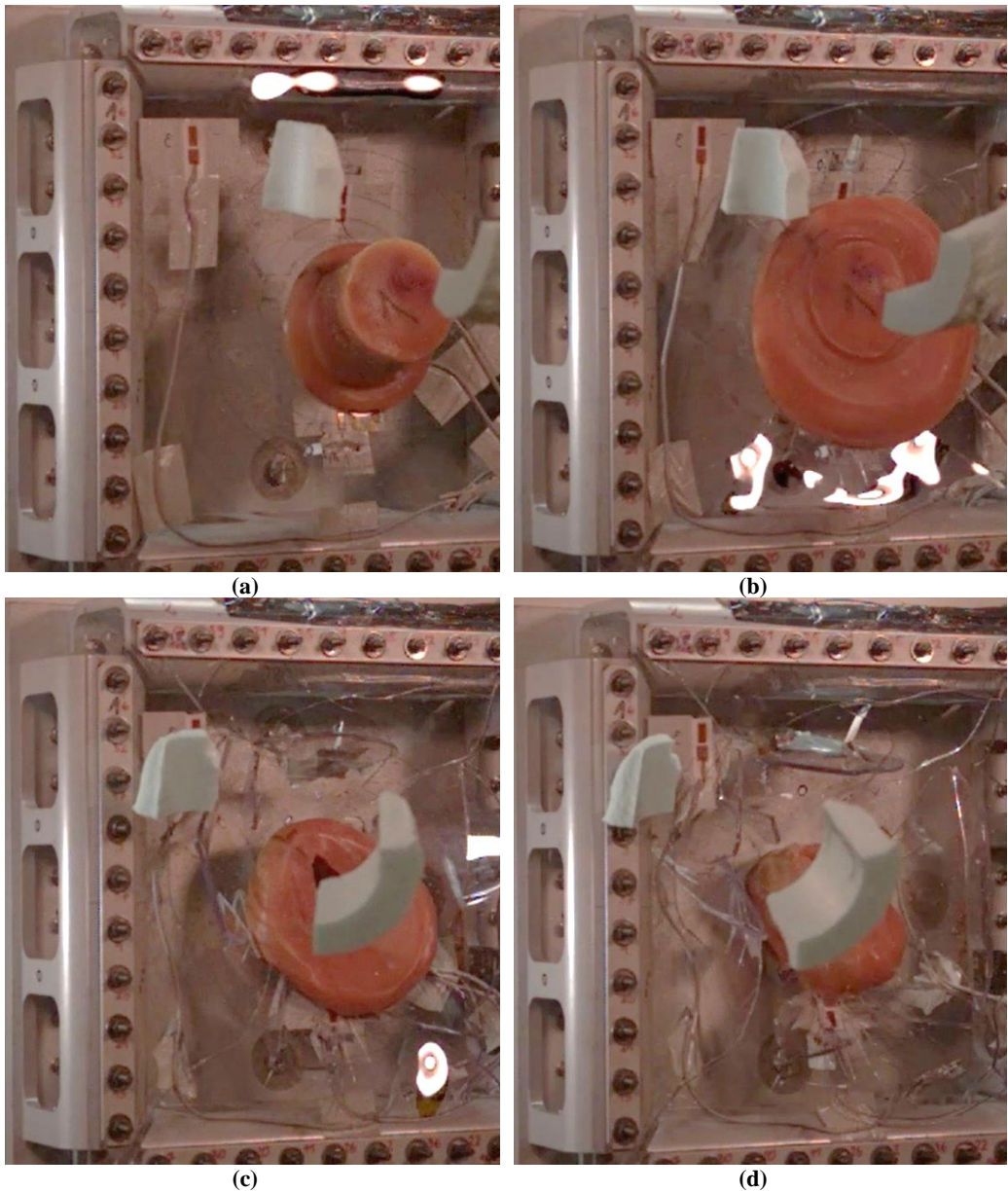


Fig. 9. Visualization of the gelatin projectile and the polycarbonate plate deformations for the impact at 50 m/s: (a) 0 ms; (b) 2. ms; (c) 3 ms (d) 4 ms

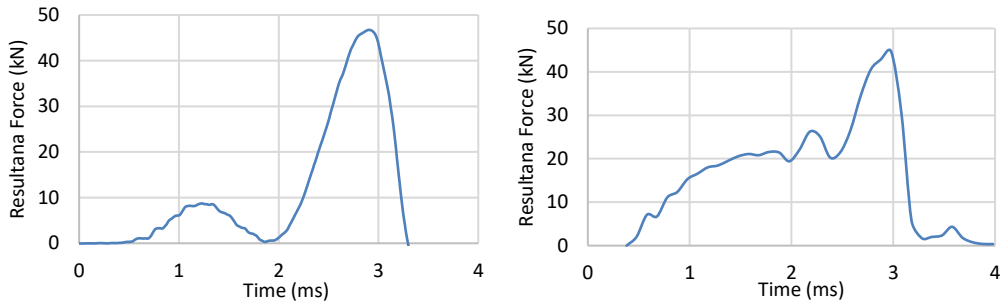


Fig. 10. Resultant force: experiment (left side), simulation (right side)

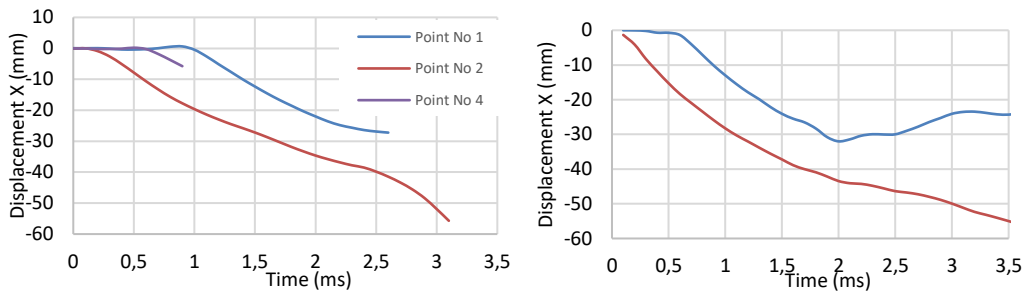


Fig. 11. Displacement of the polycarbonate sample: experiment (left side), simulation (right side)

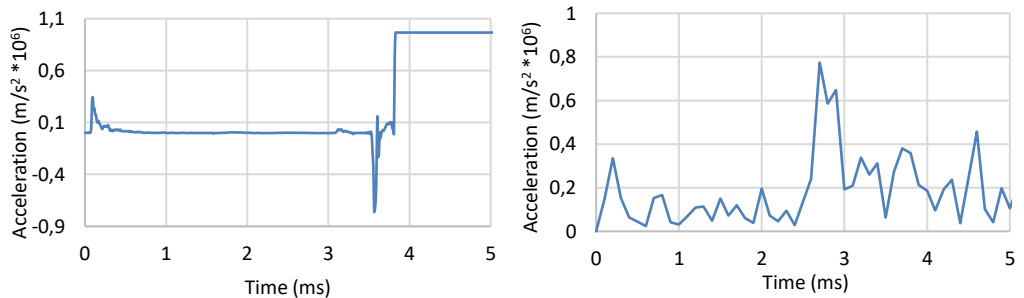


Fig. 12. Acceleration: experiment (left side), simulation (right side)

Figure 14 visualizes the gelatin projectile's impact on the windshield. Characteristic moments have been chosen to show the deformation process between the impactor and the target. It can be seen that the windshield was punctured by the impactor after about 4 ms. During a real bird strike, damaged bird bodies and pieces of the windshield can get into a cockpit and injure the crew.

Figure 15 depicts the moment the windshield got punctured, captured by a high-speed camera, and the

corresponding numerical simulation result. In Figure 16 it can be observed that the simulation reflects satisfactorily the deformation of the gelatin bird model and the effect of windshield damage during the bird impact process.

The plots of the resultant forces are presented in Figure 17. In summary, the courses of curves are similar and the maximum values of the forces are nearly the same at about 1.1 kN. The maximum force value refers to the windshield puncturing moment. After that, the forces decrease in time by about 2.5 ms and

they rise again to a value about half the maximum. It is caused by the developing damage of the windshield. As a result, the impactor loses a part of its kinetic energy. Figure 18 shows the comparison of windshield displacement between experiments and simulations.

The curve courses and the displacement values are similar. The deflection values equal about 10 mm, 15 mm, and 40 mm respectively at a time 4 ms after impact. After the shot (in a time of about 5.5 ms), as a result of this destruction, the windshield markers

were damaged too, so the displacements could not be recorded.

Figure 19 presents the comparison of accelerations recorded during the experiment and simulation. It can be seen that the courses of both curves are similar and their maximum values are similar too. This is true for the first peak which equals about 10000 g. Slight differences can be caused by the acceleration sensor's sensitivity. The peaks reference the beginning of the windshield penetration by the impactor.

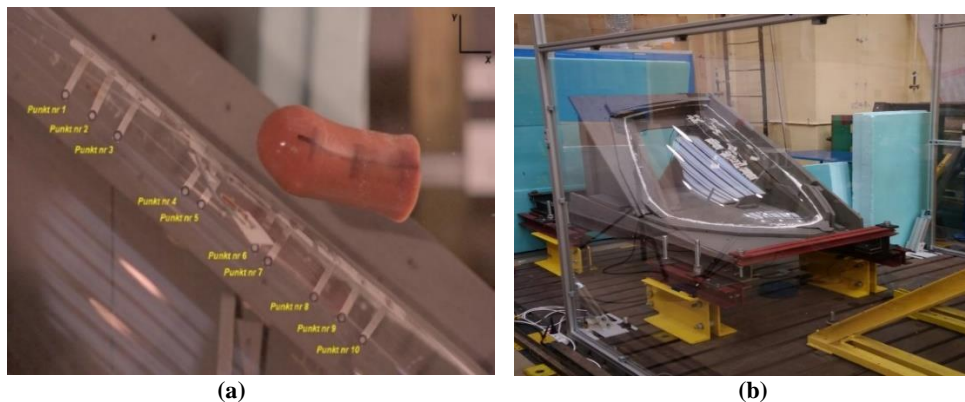


Fig. 13. Placement of markers in the windshield (a); the windshield on the test stand (b)

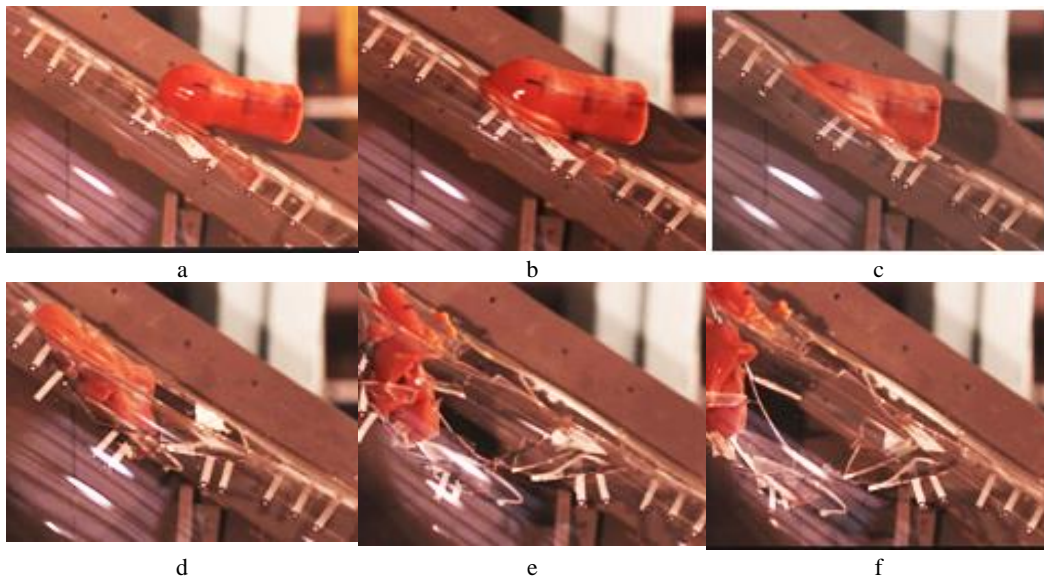


Fig. 14. Visualization of the gelatin projectile and the windshield deformations for the impact at 50 m/s: (a) 0 ms; (b) 2 ms; (c) 3 ms (d) 4ms (e) 5ms (f) 6 ms.



(a)



(b)

Fig. 15. Moment of the windshield puncturing: experiment (left side), simulation (right side)



(a)



(b)

Fig. 16. Effects of the bird model impact with the windshield: experiment (left side), simulation (right side).

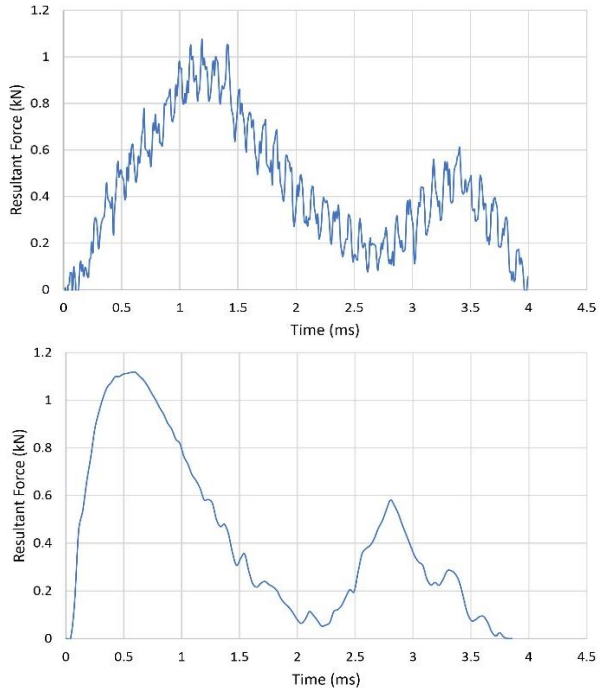


Fig. 17. Resultant force: experiment (up), simulation (down)

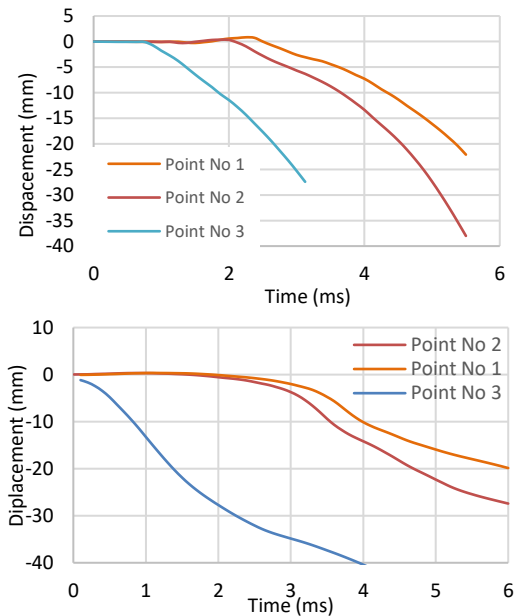


Fig. 18. Displacement of windshield: experiment (up) , simulation (down)

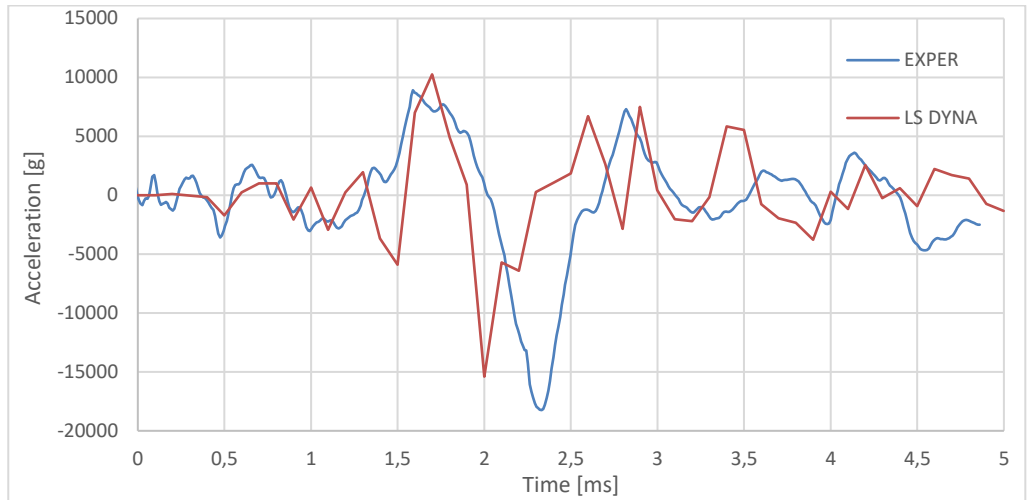


Fig. 19. Comparison accelerations recorded during experiment and simulation

5. Conclusions and Further Work

In this paper, the results of both experimental tests and numerical simulations are presented. Tests were conducted using a dedicated gas gun and a stand for fixing samples. The numerical simulations were conducted using the LS-DYNA software package. In the experiment, the gelatin projectile was the impactor, while during numerical studies the SPH bird model was used. The main aim of the investigation was the examination of polycarbonate samples and the helicopter windshield. This was to assess their strength under the impact of bird models. The mentioned research yielded some parameters of the impact process, such as force, displacement, and acceleration. Apart from that the high-speed cameras allowed visualization of the impact process. The next stage of the study was a comparison of experimental results with numerical analyses. It turned out that both the polycarbonate plate and the helicopter windshield were punctured at a speed of 50 m/s. The elaborated SPH bird model with plastic-elastic hydrodynamic material behaves well as an impactor compared to null material, especially at lower speeds such as those studied. The deformation effect of the

numerical bird model reflects satisfactorily the gelatin projectile deformation. To summarize the presented results, it is important to emphasize that the simulations conducted with L-Dyna software validate the experimental results. The presented research was the first part of the studies aimed at elaborating a bird strike-resistant windshield and other vulnerable parts of aircraft. The results of these studies may have a positive impact on air transportation safety.

Next, in experimental tests, a method of fixing sensors will be examined to determine whether the used synthetic glue weakens the windshield's structure and was a cause of puncturing. In addition, a test stand will be equipped with an additional tool that allows DIC (Digital Image Correlation) method to record displacements. Besides, one-layer and multi-layer polycarbonate samples with different thicknesses will be examined to develop windshields that are more resistant to bird strikes than those used currently.

Acknowledgements

The research was financed by the statutory research funds of the Polish Air Force University.

References

- [1] Allaey, F., Luyckx, G., Paepegem, W., Degrieck, J. (2017). Numerical and experimental investigation of shock and state pressures in the bird material during bird strike. *J. Impact Eng.* 107, 12-22. <https://doi.org/10.1016/j.ijimpeng.2017.05.006>.

- [2] Arachchige, B., Ghasemnejad, H., Yasaei, M. (2020). Effect of bird-strike on sandwich composite aircraft wing leading edge. *Adv. Eng. Softw.*, 148, 102839.
- [3] Barber, J.P. (1978). Bird impact forces and pressures on rigid and compliant targets. *Technical Report AFFDL-TR-77-60*. Air Force Flight Dynamics Laboratory, Wright-Patterson AFB OH.
- [4] Chuan, K.C. (2006). Finite Element Analysis of Bird Strikes on Composite and Glass Panels, *PhD Thesis, Department of Mechanical Engineering*, National University of Singapore.
- [5] Ćwiklak, J. (2020). The Influence of a Bird Model Shape on Bird Impact Parameters. *Facta Universitatis Series: Mech. Eng.*, 18(4), 639 – 651. <https://doi.org/10.22190/FUME200703037C>.
- [6] Ćwiklak, J., Kobińska, E., Goś, A. (2022). Experimental and numerical investigations of bird models for bird strike analysis. *Energies*, 15, 3699. <https://doi.org/10.3390/en15103699>.
- [7] Dar, U.A., Zhang, W., Xu, Y. (2013). FE analysis of dynamic response of aircraft windshield against bird impact. *Int. J. Aerospace Eng.*, 1-13. <https://doi.org/10.1155/2013/171768>.
- [8] Delsart, D., Boyer, F., Vagnot, A. (2017). Assessment of a substitute bird model for the prediction of bird-strike of helicopters structures. *In proceedings of the 7th International Conference on Mechanics and Materials in Design Albufeira*, Portugal, 997-1010.
- [9] Dennis, L., Lyle, D. (2009). Bird Strike Damage & Windshield Bird Strike Final Report. *Report European Aviation Safety Agency*.
- [10] Dhillon, B.S. (2011). *Transportation systems Reliability and safety*. Taylor and Francis Group: Boca Raton, USA. <https://doi.org/10.1201/b10729>.
- [11] Di Caprio, F., Sellitto, A., Saputo, S., Guida, M., Riccio, A. (2020). A Sensitivity Analysis of the Damage Behavior of a Leading-Edge Subject to Bird Strike, *Appl. Sci.* 10(22), 8187. <https://doi.org/10.3390/app10228187>.
- [12] Dolbeer, R.A., Begier, M.J., Miller, P.R., Weller, J.R., Anderson, A.L. (2021). *Wildlife Strikes to Civil Aircraft in the United States, 1990–2020*. Federal Aviation Administration: Washington, DC, USA.
- [13] El-Sayed, A.F. (2019). *Bird Strike in Aviation: Statistics, Analysis and Management*. John Wiley & Sons: Hoboken, NJ, USA.
- [14] Fragassa, C., Topalovic, A., Pavlovic, A., Vulovic, S. (2019). Dealing with the Effect of Air in Fluid Structure Interaction by Coupled SPH-FEM Methods. *Materials* 12(7), 1162. <https://doi.org/10.3390/ma12071162>.
- [15] Guida, M., Marulo, F., Meo, M., Grimaldi, A., Olivares, G. (2011). SPH Lagrangian study of bird impact on leading edge wing. *Compos. Struct.*, 93(3): 1060e–71. <https://doi.org/10.1016/j.compstruct.2010.10.001>.
- [16] Guida, M., Marulo, F., Meo, M., Russo, S. (2013). Certification by birdstrike analysis on C27J full scale ribless composite leading edge, *Int. J. Impact Eng.*, 54, 105-113. <https://doi.org/10.1016/j.ijimpeng.2012.10.002>.
- [17] Hedayati, R., Sadighi, M. (2015). *Bird Strike: An Experimental, Theoretical and Numerical Investigation*. Woodhead Publishing: Cambridge, UK.
- [18] Hedayati, R., Ziaei-Rad, S. (2012). A new bird model and Effect of bird geometry and orientation on bird-target impact analysis using SPH method. *Int. J. Crashworthiness*, 17(4), 445-459. <https://doi.org/10.1080/13588265.2012.674333>.
- [19] Hedayati, R., Ziaei-Rad, S., Eyvazian, A., Hamouda, A.M. (2014). Bird strike analysis on a typical helicopter windshield with different lay-ups. *J. Mech. Scien. Tech.*, 28(4), 1381-1392. <https://doi.org/10.1007/s12206-014-0125-3>.
- [20] Heimbs, S. (2011). Bird Strike Simulations on Composite Aircraft Structures. *In Proceedings of the Simulia Customer Conference*, Barcelona, Spain, 1-13.
- [21] Heimbs, S. (2011). Computational methods for bird strike simulations: A review. *Comput. Struct*, 89, 2093–2112. <https://doi.org/10.1016/j.compstruc.2011.08.007>.
- [22] Husainie, S.N. (2017). Bird Strike and Novel Design of Fan Blades. *In Proceedings of the Science in the Age of Experience*, Chicago, Illinois.

- [23] Ivančević, D., Smojver, I. (2011). Hybrid Approach in Bird Strike Damage Prediction on Aeronautical composite structures. *Compos. Struct*, 94(1), 15-23. <https://doi.org/10.1016/j.compstruct.2011.07.028>.
- [24] Jin, Y. (2018). A review of research on bird impacting on jet engines. In Proceedings of the IOP Conference Series: *Materials Science and Engineering*, Kuala Lumpur, Malaysia, 012014.
- [25] Kalam, A., Kumar, R., Ranga Janardhana, G. (2017). SPH High Velocity Impact Analysis-Influence of Bird Shape on Rigid Flat Plate, *Materials Today*, 4(2), Part A, 2564–2572. <https://doi.org/10.1016/j.matpr.2017.02.110>.
- [26] Lacombe, J.L. (2004). Smoothed particle hydrodynamics method in LS-DYNA. In *3rd German LS-DYNA forum*, Bamberg, Germany, 7-33.
- [27] Liu, J., Li, Y., Gao, X. (2014). Bird strike on a flat plate: Experiments and numerical simulations. *Int. J. Impact Eng.*, 70, 21–37. <https://doi.org/10.1016/j.ijimpeng.2014.03.006>.
- [28] Liu, J., Yulonga, L., Xiaoshengb, G., Xiancheng, Y. (2014). A numerical model for bird strike on side wall structure of an aircraft nose, *Chin. J. Aeronaut*, 27(3), 542-549. <https://doi.org/10.1016/j.cja.2014.04.019>.
- [29] Livermore Software Technology Corporation, (2007), *LS-DYNA Keyword User's Manual*, USA.
- [30] Lyu, H-G., Sun P-N., Huang, X-T., Zhong, S-Y., Peng, Y-X., Jiang, T., Ji, C-N. (2022). A Review of SPH Techniques for Hydrodynamic Simulations of Ocean Energy Devices. *Energies*, 15(2), 502. <https://doi.org/10.3390/en15020502>.
- [31] McCarthy, M.A., Xiao, R.J., McCarthy, C.T., Kamoulakos, A., Ramos, J., Gallard, J.P. (2010). Melito V. Modeling Bird Impacts on an Aircraft Wing- Part 2 Modeling the impact with and SPH bird model. *Int. J. Crashworthiness*, 10(1), 51-59. <https://doi.org/10.1533/ijcr.2005.0325>.
- [32] McIntyre, G.R. (2017). Patterns In Safety Thinking. *A literature Guide to Air Transportation Safety*. Taylor and Francis Group: London, UK. <https://doi.org/10.4324/9781315247281>.
- [33] Metz, I., Ellerbroek, J., Mühlhausen, T., Kügler, D., Kern, S., Hoekstra, J. (2021). The Efficacy of Operational Bird Strike Prevention, *Aerospace*, 8(1), 17. <https://doi.org/10.3390/aerospace8010017>.
- [34] Orlando, S., Marulo, F., Guida, M., Timbrato, R. (2018). Bird strike assessment for a composite wing flap. *Int. J. Crashworthines*, 23, 219-235. <https://doi.org/10.1080/13588265.2017.1342521>.
- [35] Pernas-Sánchez, J., Artero-Guerrero, J., Varas, D., López-Puente, J. (2020). Artificial bird strike on Hopkinson tube device: Experimental and numerical analysis. *Int. J. Impact Eng.*, 138, 103477. <https://doi.org/10.1016/j.ijimpeng.2019.103477>.
- [36] Plassarda, F., Hereil, P., Pierric, J., Mespoulet, J. (2015). Experimental and numerical study of a bird strike against a windshield. *European Physical Journal Web of Conferences*, 94, 01051. <https://doi.org/10.1051/epjconf/20159401051>.
- [37] Regulation EASA (2022). CS-25, Certification Specifications for Large Aeroplanes, *Amdt 11*, EASA 2011. <https://www.easa.europa.eu/document-library/certification-specifications/cs-25-amendment-11>.
- [38] Regulation EASA (2022). CS-29, Certification Specifications for Large Rotorcraft, *Amdt 11*, EASA 2011. <https://www.easa.europa.eu/document-library/certification-specifications/cs-29-amendment-11>.
- [39] Ropero-Giralda, P., Crespo, A.J.C., Coe, R.G., Tagliaferro, B., Domínguez, J.M., Bacelli, G., Gómez-Gesteira, M. (2021). Modelling a Heaving Point-Absorber with a Closed-Loop Control System Using the DualSPHysics Code. *Energies*, 14, 760. <https://doi.org/10.3390/en14030760>.
- [40] Soni, C., Katukam, R. (2013). Bird Strike Analysis of an Airframe, Comparison of Methods and Validation. In *proceedings of the Simulia India Regional User Meeting* 13, 1-14.
- [41] Vijayakumar, R., Gulbarga, K., Ravindranath, R. (2015). Bird strike simulation on composite structures. In *Proceedings of the 41st European Rotorcraft Forum Munich*, German.
- [42] Wang, F.S., Yue, Z.F. (2010). Numerical simulation of damage and failure in aircraft windshield structure against bird strike. *Mater Des.*, 31(2), 687–95. <https://doi.org/10.1016/j.matdes.2009.08.029>.
- [43] Wilbeck, J.S. (1977). Impact Behavior of Low Strength Projectiles, *Technical Report AFML-TR-77-134*, Air Force Materials Laboratory, Wright-Patterson AFB OH.

- [44] Wu, B., Lin, J., Hedayati, R., Zhang, G., Zhang, J., Zhang, L. (2021). Dynamic responses of the aero-engine rotor system to bird strike on fan blades at different rotational speeds. *Appl. Sci.*, 11, 8883. <https://doi.org/10.3390/app11198883>.
- [45] Yang, J., Cai, X., Wu, C. (2003). Experimental and FEM study of windshield subjected to high speed bird impact. *Acta Mech Sinica*, 19(6), 543–50. <https://doi.org/10.1007/BF02484547>.
- [46] Zhang, Z., Li, L., Zhang, D. (2018). Effect of arbitrary yaw/pitch angle in bird strike numerical simulation using SPH method. *Aerosp. Sci. Technol.*, 81, 284–293. <https://doi.org/10.1155/2021/8879874>.
- [47] Zhou, Y., Sun, Y., Huang, T. (2020). Bird-Strike Resistance of Composite Laminates with Different Materials. *Materials*, 13(1), 129. <https://doi.org/10.3390/ma13010129>.
- [48] Zhou, Y., Sun, Y., Huang, T. (2019). SPH-FEM Design of Laminated Plies under Bird-Strike Impact. *Aerospace*, 6(10), 112. <https://doi.org/10.3390/aerospace6100112>.
- [49] Zhu, S., Wu, C., Yin, H. (2021). Virtual Experiments of Particle Mixing Process with the SPH-DEM Model. *Materials*, 14(9), 2199. <https://doi.org/10.3390/ma14092199>.
- [50] Zochowski, P., Bajkowski, M., Grygoruk, R., Magier, M., Burian, W., Pyka D., Bocian, M., Jamroziak, K. (2022). Comparison of Numerical Simulation Techniques of Ballistic Ceramics under Projectile Impact Conditions. *Materials*, 15(1), 18. <https://doi.org/10.3390/ma15010018>.